Semiconductor Materials

DOI: 10.1002/ange.200603075

# A Crystalline, Large-Pore, Microporous Semiconductor**

*Alexander Shulman and Anders E. C. Palmqvist**

Crystalline, microporous semiconductors are of interest for a variety of potential applications, such as chemical sensors, electro-optics, thermoelectrics, and low-dimensional electronics. Over the past two decades research has been devoted to discovering naturally occurring and synthetic microporous materials with semiconducting properties. Simon et al., for example, have reported a synthetic cetineite analogue with the composition $|K_6(H_2O)_6|[Sb_{12}O_{18}][SbSe_3]_2$, which was described to be the first crystalline, microporous material of this family of materials to feature a photo-semiconducting host structure and a band gap of 2060 meV.[1]

A variety of additional synthetic cetineite-type phases also reveal optical band gaps in the visible range and electrical semiconductivities.[2] Experimental results[1,3] and theoretical computations[3] have demonstrated that the optical band gaps of the members of the cetineite family with the general formula $A_6[Sb_{12}O_{18}][SbX_3]_2$ (A = K or Na, X = S or Se) vary with the composition of the crystal and tend to decrease with increasing atomic number of both the alkali metal and the chalcogen. It was suggested that these properties may be attributed to an overlap of the sp, $d_{xz}$, and $d_{yz}$ orbitals of the Sb atoms of chemically different subunits (namely the $\{Sb_{12}O_{18}\}$ tubular unit and the $\{SbS_3\}^{3-}$ or $\{SbSe_3\}^{3-}$ pyramids) in an alternating sequence along the crystallographic *c* axis.[3,4]

Recently, a crystalline, microporous, semiconducting antimony(III) oxide telluride known as K-SBC-1 has been synthesized.[5] K-SBC-1 is structurally related to the cetineite family as it shares the $\{Sb_{12}O_{18}\}$ tubular unit, but it differs in that it has a tellurium tubular unit instead of the network of pyramidal $\{SbX_3\}^{3-}$ anions enclosing the $\{Sb_{12}O_{18}\}$ units. The structure of K-SBC-1 is also of interest from a structural classification point of view since it consists of guests within a host within a second host and thus appears to be the first example of a second-order zeoate according to the recent suggestion for the extension of the nomenclature of microporous materials.[6] The strongly reduced crystal chemical formula of K-SBC-1 is $|(|K_6(H_2O)_6|[Sb_{12}O_{18}])_3|[Te_{36}]$, and this crystalline microporous material is a narrow-band-gap semiconductor with a band gap of only 250 meV and a highly anisotropic and relatively large electrical conductivity.[5]

As a result of our recent investigations of the related rubidium antimony(III) oxide telluride system, we now report a new crystalline, large-pore, microporous semiconductor. The structure, referred to as Rb-CTH-1, is related to K-SBC-1 and the cetineite and exhibits a number of fascinating structural features and properties. For instance, isolated Rb ions are hosted by a unique 18-ring $\{Sb_{18}O_{27}\}$ tubular unit which, in turn, is surrounded by an intricate, ordered network built up from trigonal pyramidal $\{SbTe_3\}^{3-}$ anions and $Te_2^{2-}$ dumbbells. The overall reduced crystal chemical formula of Rb-CTH-1 is $|Rb_{18}|[Sb_{36}O_{54}][(SbTe_3)_2(Te_2)_6]$ and the structure is classified as a first-order zeoate following the most recent suggestion for this new nomenclature.[6] In addition, Rb-CTH-1 has a band gap of 850 meV, which makes it interesting for applications within the domain of microporous semiconductors.

Dark-red, acicular crystals of Rb-CTH-1 with a length of 0.1–2 mm and a diameter of approximately 0.03–0.1 mm (shown in Figure 1) were formed over seven days by solvothermal treatment of a reagent mixture with the molar ratio $Te/Sb/Rb_2O/C_3H_7NH_2/H_2O$ 1:0.682:0.774:0.68:19.35 at 453 K. The yield of product ranged from 1–60 vol% depending on the orientation of the autoclave in the oven. Syntheses in vertically positioned autoclaves typically produced extremely low yields of Rb-CTH-1 of approximately

[*] Prof. A. E. C. Palmqvist
Department of Chemical and Biological Engineering
Applied Surface Chemistry and Competence Centre for Catalysis
Chalmers University of Technology, 41296 Göteborg (Sweden)
Fax: (+46) 31-160-062
E-mail: adde@chalmers.se

A. Shulman
Department of Chemical and Biological Engineering
Applied Surface Chemistry
Chalmers University of Technology
41296 Göteborg (Sweden)

[**] Financial support from the Swedish Research Council and the Carl Trygger Foundation is greatly appreciated. Dr. Vratislav Langer, Göteborg, and Dr. Jacob Overgaard, Aarhus, are acknowledged for technical assistance during the single-crystal diffraction data collection and absorption correction of the obtained datasets. Dr. Ezio Zanghellini, Göteborg, is acknowledged for his assistance during the DRIFT analysis. Prof. Susan Jagner, Göteborg, and Dr. Rasmus Damgaard Poulsen, Aarhus, are thanked for valuable discussions.

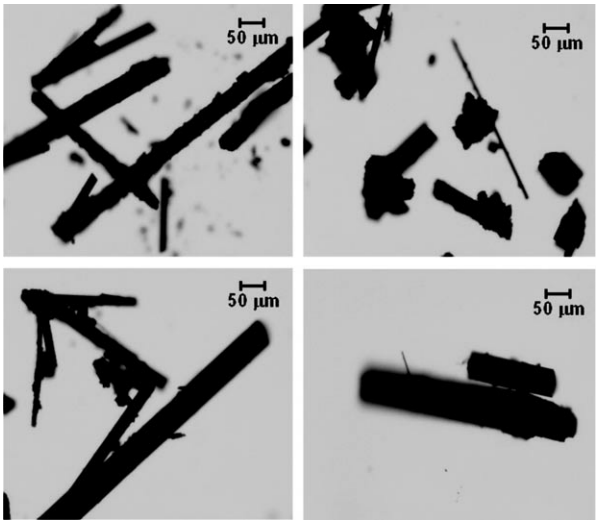


***Figure 1.*** Photographs of collections of Rb-CTH-1 crystals.

1 vol %. Such low yields appear to be linked to the fact that the interfacial area between the gas, liquid, and solid phases, and therefore the contact area available for secondary nucleation, are lower under these conditions than in horizontally positioned autoclaves. Syntheses in the latter yielded up to 60 vol % of Rb-CTH-1. The main impurities were identified as $Sb_2Te_3$, $Sb_{0.405}Te_{0.595}$, $Te_2O_5$, and traces of $Te(OH)_6$.

The crystal structure of Rb-CTH-1 is presented in Figure 2. Rb-CTH-1 grows in the hexagonal space group $P6_3/mmc$ (no. 194) with hexagonal axes, and $a = b = 21.8578(2)$ and $c = 9.7599(2)$ Å at 295 K. The structure contains a unique 18-ring $\{Sb_{18}O_{27}\}$ tubular unit (see Figure 2 a,b) with a ring width of $13.12 \times 13.49$ Å (assuming a van der Waals radius, $r(O)$, of 1.35 Å). The unit resembles the $\{Sb_{12}O_{18}\}$ 12-ring tubular unit in K-SBC-1 and the cetineites in that it is built up from pyramidal $\{SbO_3\}$ groups linked together through common oxygen atoms and hosts alkali-metal ions, in this case rubidium ions. The distance between the Sb and O atoms in the $\{SbO_3\}$ groups ranges from 1.965 to 2.018 Å.

The walls of the $\{Sb_{18}O_{27}\}$ unit consist of $\{Sb_6O_6\}$ rings. Unlike K-SBC-1, where all the $\{Sb_6O_6\}$ rings are alike, Rb-CTH-1 features two different types of $\{Sb_6O_6\}$ rings. Ring A has a ring width of $2.88 \times 2.88 \times 2.98$ Å ($r(O) = 1.35$ Å) and consists of the following antimony atoms named in clockwise order: SB2, SB2, SB1, SB1, SB1, and SB1. Ring B has a ring width of $2.75 \times 3.01 \times 3.01$ Å ($r(O) = 1.35$ Å) and is built up from the following antimony atoms, also listed clockwise: SB1, SB1, SB2, SB1, SB1, and SB2. These dimensions are comparable in size to the $\{Sb_6O_6\}$ rings in K-SBC-1, which have a ring width of $2.73 \times 2.88 \times 2.99$ Å.[5] The 6-rings coordinate the rubidium ions in a manner similar to crown ethers, with the six distances between the rubidium ion and the oxygen atoms ranging from 2.986 to 3.049 Å for ring A and from 2.946 to 3.406 Å for ring B.

Although unique in its configuration, the outer network consists of well-known building blocks. The trigonal pyramidal $\{SbTe_3\}^{3-}$ anions are found, for example, in clathrates, such as $Na_3SbTe_3$[7] and $K_3SbTe_3$,[8] and interestingly enough, pyramidal $\{SbS_3\}^{3-}$ and $\{SbSe_3\}^{3-}$ anions have been found in the cetineite structure,[1–4] although the $\{SbTe_3\}^{3-}$ anion has not. The Sb–Te distance in the $\{SbTe_3\}^{3-}$ anions in Rb-CTH-1 is 2.726 Å, which is somewhat shorter than those in $Na_3SbTe_3$ and $K_3SbTe_3$ (2.783 and 2.787 Å, respectively). The Te–Sb–Te angle in the $\{SbTe_3\}^{3-}$ anions in Rb-CTH-1 is 95.45° (100.0° in $Na_3SbTe_3$ and 101.9° in $K_3SbTe_3$). In agreement with the investigation of bond and atomic valences in chalcogen compounds,[9] the value of the Te–Sb–Te angle suggests that the effective valence of the Sb atom lies close to +3. The distortion from the regular tetrahedral angle (109.5°) can thus be assigned to the effect of the lone electron pair (LEP) at each $Sb^{3+}$ site, as previously discussed in the literature.[7]

Similar to the Sb–S and Sb–Se bonds in the cetineites, the Sb–Te bond in Rb-CTH-1 is expected to be rigid due to its considerable degree of covalency. Structure refinements reveal an orientational disorder of the $\{SbTe_3\}^{3-}$ anions. The $\{SbTe_3\}^{3-}$ anions in the tubular interstices are stacked either parallel or antiparallel to [001], and all the pyramids in a single interstice are expected to have the same orientation in the $c$ direction since the strong repulsive forces between the

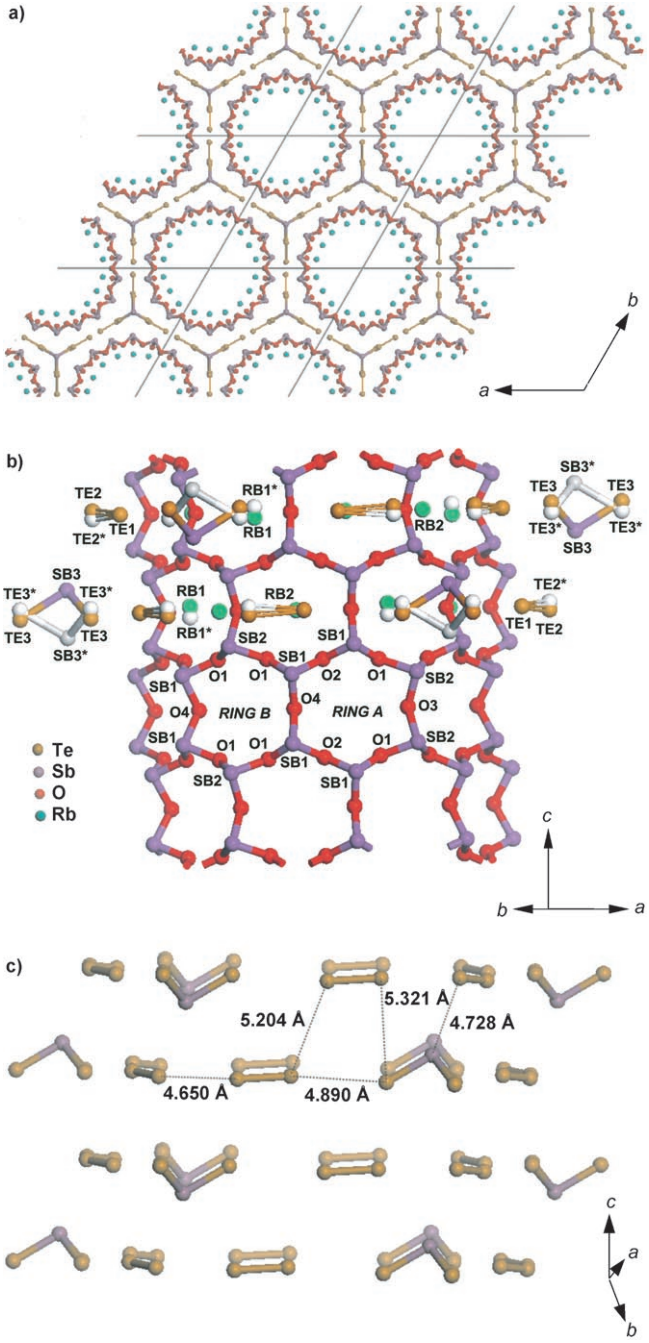


***Figure 2.*** Structure of Rb-CTH-1: a) Projection onto the (001) plane showing isolated $Rb^+$ ions hosted by a $\{Sb_{18}O_{27}\}$ tubular unit which, in turn, is placed within a complex network consisting of trigonal pyramidal $\{SbTe_3\}^{3-}$ anions and $Te_2^{2-}$ dumbbells; b) a side front view of a $\{Sb_{18}O_{27}\}$ tubular unit with $Rb^+$ ions as guests and the outer arrangement of disordered trigonal pyramidal $\{SbTe_3\}^{3-}$ anions and $Te_2^{2-}$ dumbbells. $Rb^+$ ions, $\{SbTe_3\}^{3-}$ pyramids, and $Te_2^{2-}$ dumbbells have been removed in the lower part of the figure for clarity; this enables the location of the assigned atoms and rings in the $Sb_6O_6$ units to be seen more clearly. Alternative positions for disordered atoms are marked with an asterisk; c) a side view of a network containing trigonal pyramidal $\{SbTe_3\}^{3-}$ anions and $Te_2^{2-}$ dumbbells surrounding the $\{Sb_{18}O_{27}\}$ tubular unit. The $\{Sb_{18}O_{27}\}$ unit and the disordered atoms/groups have been removed for clarity.

  

LEPs at the Sb atoms would prevent them from having opposite orientations. The orientation of the $\{SbTe_3\}^{3-}$ anions is expected to vary randomly from one interstice to another. This structural peculiarity is also observed in the cetineites.[10,11]

The Te atoms in the $\{SbTe_3\}^{3-}$ anions do not lie on special positions—the deviation of the split position of the Sb and Te atoms in the $\{SbTe_3\}^{3-}$ anion from the mirror plane parallel to (001) is 1.18 and 0.24 Å, respectively.

$Te_2^{2-}$ dumbbells are also encountered in a variety of structures, such as K-SBC-1,[5] $ThTe_2I_2$,[12] and $BaBiTe_3$.[13] The Te–Te distance in a $Te_2^{2-}$ dumbbell is 2.727 Å in Rb-CTH-1, which is somewhat shorter than the values of 2.784 Å found in K-SBC-1[5] and 2.864 Å in elemental tellurium. The Te atom that lies closest to the $\{SbTe_3\}^{3-}$ anion in the $Te_2^{2-}$ dumbbells in Rb-CTH-1 also exhibits orientational disorder, with a deviation of the split position from the mirror plane parallel to (001) of 0.191 Å. This disorder appears to be caused by repulsion between the LEP on the Sb atom in the anion and the electron cloud of the Te atom in the dumbbell. Hence, the orientation of the dumbbell in the *c* direction is expected to be similar to that of the neighboring $\{SbTe_3\}^{3-}$ anion.

When projected normal to (001), the arrangement is seen to be composed of layers, each of which consists of six dumbbells and three $\{SbTe_3\}^{3-}$ anions (see Figure 2c). This network is clearly not closed since the separations between the building blocks of the network exceed the van der Waals bond distance of 4.12 Å for a Te–Te interaction.

The $Te_2^{2-}$ dumbbells and the $\{SbTe_3\}^{3-}$ anions are located on the opposite sides of the $\{Sb_6O_6\}$ rings of the $\{Sb_{18}O_{27}\}$ tube walls to the rubidium ions. An interesting feature of the Rb-CTH-1 structure is the position of the $\{SbTe_3\}^{3-}$ anions and the $Te_2^{2-}$ dumbbells with respect to the two types of $\{Sb_6O_6\}$ rings and to the two crystallographically different kinds of rubidium ions. Apparently, the $Te_2^{2-}$ dumbbells lie on the opposite side of $\{Sb_6O_6\}$ rings of type A from RB2 cations, whereas the $\{SbTe_3\}^{3-}$ anions lie opposite to $\{Sb_6O_6\}$ rings of type B, which coordinate RB1 cations. The two Te atoms in a dumbbell are not symmetrically located with respect to the center of the ring of type A, with a separation between these Te atoms and the rubidium cation of 4.353 and 4.944 Å, respectively.

The $\{SbTe_3\}^{3-}$ anions lie symmetrically with respect to the center of an $\{Sb_6O_6\}$ ring of type B. As a consequence of the orientational disorder exhibited by the $\{SbTe_3\}^{3-}$ anions, the rubidium cation RB1 located on the opposite side of the $\{Sb_6O_6\}$ ring of type B may occupy two positions, each of which lies symmetrically with respect to the mirror plane parallel to (001), with a separation of 0.264 Å from the latter. The position occupied by the cation is clearly directed by the orientation of the $\{SbTe_3\}^{3-}$ anion. Apparently, the stacking of the anions parallel to [001] causes the rubidium cations to occupy a position above the mirror plane, whereas for antiparallel stacking of the anions the coordinated rubidium cations occupy positions below the mirror plane. The distance between the two Te atoms pointing inward to the rubidium cation located on the opposite side of the $\{Sb_6O_6\}$ ring is 5.348 Å.

Unlike K-SBC-1 and the cetineites no ordered guest species other than the metal counter cations are encountered inside the antimony(III) oxide tubular unit of Rb-CTH-1, thereby suggesting that this structure may have a larger sorption capacity. However, some residual electron density found inside the $\{Sb_{18}O_{27}\}$ tubular unit may be evidence for the presence of disordered water or template molecules residing inside the tube. Owing to the larger tube diameter in Rb-CTH-1 compared to the cetineites and to K-SBC-1, the mobility of these molecules inside the tubes is expected to be higher in the former, which causes these molecules to be disordered in the 1D channels of the structure.

In agreement with the IUPAC nomenclature for porous solids, Rb-CTH-1 should be classified as a microporous material similar to the structurally related cetineites and K-SBC-1.[6,14–16] It is, however, still unclear whether the structural integrity would remain intact upon removal of the guest species and hence it is uncertain whether Rb-CTH-1 would exhibit any porosity in the more applied meaning of the word, that is, the ability to demonstrate reversible sorption and ion-exchange.

Generally, it is difficult to distinguish between tellurium and antimony in the $\{SbTe_3\}^{3-}$ anions by X-ray diffraction alone because of the similar scattering cross-sections for X-rays for these elements. However, the Sb–Te bond distance and the Te–Sb–Te angle in the $\{SbTe_3\}^{3-}$ anions confirm that the position at the top of the pyramid is in fact occupied by an antimony atom. Furthermore, simple electron-counting arguments strongly support that the crystal chemical formula for Rb-CTH-1 is $|Rb_{18}|[Sb_{36}O_{54}][(SbTe_3)_2(Te_2)_6]$. The Sb in the $\{Sb_{18}O_{27}\}$ tubes is expected to have the same oxidation state as in K-SBC-1,[5] that is +3, which means that the $\{Sb_{18}O_{27}\}$ tubes are charge neutral. Tellurium is known to have mixed oxidation states in polytellurides.[17] The average Te oxidation state in K-SBC-1, for instance, is −0.5,[5] whereas it is expected to be $-1^1/_3$ in Rb-CTH-1.

Similar to the case of cetineites[1–4,10] and K-SBC-1,[5] the $\{Sb_{18}O_{27}\}$ tubes are presumably stabilized by the strong Sb–O bonds, whereas the overall structure is held together by ionic forces between the negatively charged $\{SbTe_3\}^{3-}$ pyramids and $Te_2^{2-}$ dumbbells in the tubular interstices, and the rubidium counter cations lined on the inside of the $\{Sb_{18}O_{27}\}$ tubes.

As it is structurally and compositionally similar to the members of the cetineite family and to K-SBC-1, Rb-CTH-1 was expected to exhibit semiconducting properties. The diffuse reflectance spectrum of Rb-CTH-1 is shown in Figure 3. A series of bands are found below 250 meV associated with the optical vibrational modes of the crystal structure. A broad band centered around 405 meV is associated with OH stretching modes, which are apparently due to adsorbed molecular water in the sample structure. The measurements demonstrate that Rb-CTH-1 has a forbidden band below 660 meV, where photons are absorbed solely by exciting the vibrational modes of the system. Above approximately 660 meV, the steep rise in the absorption of the sample is evidence for the presence of a conduction band. Some spurious features are observed at about 350–360 and 790 meV. These arise from CH contamination of the beam

  

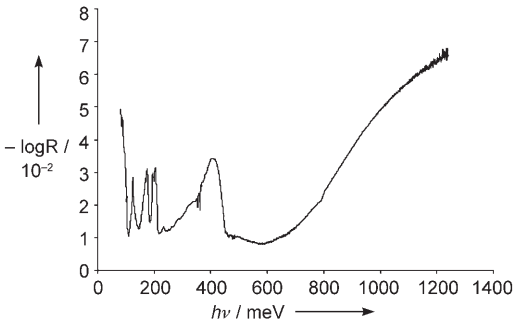


***Figure 3.*** The diffuse reflectance spectrum of an Rb-CTH-1 sample ground with KCl showing the logarithm of the inverse reflectance as a function of photon energy.

splitter in the former case and a small drift of the response of the germanium diode detector in the latter.

It is not obvious from the spectrum where the steep rise ends and therefore it is not very clear exactly how large the band gap is. The rise itself is much broader than 50 meV ($k_BT$ for $T$ of about 300 K), therefore it is intrinsic to the structure and is not simply a consequence of thermal effects.[18] The derivative of the steep rise is almost constant over quite a broad range (more than five times $k_BT$).

Despite the fact that the logarithm of the inverse reflection does not precisely match the real absorption spectrum, the former is often used to estimate the latter when the nature of the sample or the measurement techniques do not allow for collection of the real absorption spectrum. It has been reported that band-gap energies in semiconducting materials can be evaluated directly from the absorption spectrum with an accuracy of 5 meV.[19] Thus, the band-gap energy in Rb-CTH-1 was estimated to be 850 meV from the derivative spectrum of the inverse logarithmic reflectance with respect to the photon energy.

In conclusion, a new crystalline, large-pore, microporous semiconductor (Rb-CTH-1) has been prepared by means of solvothermal synthesis. Its structure was determined by single-crystal X-ray diffraction. The material possesses several unique structural features, such as an 18-ring $\{Sb_{18}O_{27}\}$ tubular unit that was previously unknown in any chemical compound. The antimony(III) oxide tubular unit is surrounded by an intricate, ordered arrangement consisting of trigonal pyramidal $\{SbTe_3\}^{3-}$ anions and $Te_2^{2-}$ dumbbells. Some positive residual electron density inside the $\{Sb_{18}O_{27}\}$ tubular unit presumably arises from disordered guest species occupying the tube. The nature of these species is difficult to determine, although the diffuse reflectance spectroscopy analysis indicates the presence of water in the structure. DRIFT measurements also reveal a band gap of 850 meV, thus making Rb-CTH-1 interesting for applications typical for materials in the domain of crystalline, microporous semiconductors.

## *Experimental Section*

Crystallization of Rb-CTH-1 was effected batch-wise by solvothermal treatment of a reagent mixture containing elemental antimony (99.999%, crushed pieces, freshly ground), tellurium (99.999%, crushed pieces, freshly ground), *n*-propylamine (98%), rubidium hydroxide (99.9% as 50 wt% solution in water), and deionized water. All reagents used, except for the deionized water, were purchased from Aldrich.

The procedure used for preparation of Rb-CTH-1 was as follows. The reagents were weighed and placed in a 45-mL, Teflon-lined, stainless-steel autoclave (Parr Instrument Corp.). The autoclave was vigorously shaken for approximately 1 min and then placed in an oven at 453 K. The autoclave was typically quenched in air at ambient temperature after seven days of heat treatment. The liquid phase was separated from the solid phase by filtration, and the solid product was washed with ethanol and dried in air. Rb-CTH-1 formed as dark-red, acicular crystals, which were manually separated from the rest of the solid material and placed in sealed glass vials. The yield of Rb-CTH-1 in the product mixture was estimated visually.

The crystal structure of Rb-CTH-1 was determined at 298 K using a Siemens SMART CCD single-crystal X-ray diffractometer ($Mo_{K\alpha}$ radiation, $\lambda = 0.71073$ Å). Data collection and integration were carried out using the SMART software. Averaging and absorption correction were done using SADABS. Structure solution and refinement were performed using the WinGX v1.70.01 program package.[20] Rb-CTH-1: hexagonal, $P6_3/mmc$ (no. 194), $a = b = 21.8578(2)$, $c = 9.7599(2)$ Å at 298 K. $V = 4038.21(1)$ Å$^3$, $25 \times 30 \times 440$ μm, $\rho_{calcd} = 3.840$ g cm$^{-3}$, $2\theta_{max} = 58.24°$, $\lambda = 0.71073$ Å, $\mu = 14.88$ mm$^{-1}$; number of measured reflections: 55726; number of unique reflections included in the refinement: 1958; least-squares refinement: $N_{par} = 66$, $R(\text{int}) = 0.1016$, $R(\sigma) = 0.0271$, $R1 = 0.0639$ refined against $|F|$, $wR2 = 0.1231$ and GooF $= S = 1.055$ refined against $|F^2|$. Further details of the crystal structure investigations may be obtained from the Fachinformationszentrum Karlsruhe, 76344 Eggenstein-Leopoldshafen, Germany (fax: (+49) 7247-808-666; e-mail: crysdata@fiz-karlsruhe.de), on quoting the depository number CSD-416106.

FTIR spectroscopy analysis of Rb-CTH-1 was performed in a diffuse-reflectance (DR) geometry to investigate the optical properties of the material. A small amount of Rb-CTH-1 was ground together with KCl in an agate mortar in a ratio of about 1 to 50 in volume. A similar sample of pure KCl was used as reference. The measurements were performed on a Bruker IFS 66v/S FTIR instrument, using a Graseby Specac diffuse reflection unit, model Selector. The signal in the mid-IR region (650–5700 cm$^{-1}$ or 80–710 meV) was detected using a KBr beam-splitter and an MCT detector. The signal in the near-IR region (5700–10000 cm$^{-1}$ or 710–1200 meV) was detected using a quartz beam-splitter and a germanium diode detector.

Received: July 29, 2006
Revised: October 30, 2006
Published online: December 8, 2006

**Keywords:** antimony · microporous materials · semiconductors · tellurium · zeolite analogues

[1] U. Simon, F. Schüth, S. Schunk, X. Wang, F. Liebau, *Angew. Chem.* **1997**, *109*, 1138; *Angew. Chem. Int. Ed. Engl.* **1997**, *36*, 1121.
[2] F. Liebau, X. Wang, *Eur. J. Mineral.* **1997**, *9*, 223.
[3] F. Starrost, E. E. Krasovskii, W. Schattke, J. Jockel, U. Simon, X. Wang, F. Liebau, *Phys. Rev. Lett.* **1998**, *80*, 3316.
[4] U. Simon, V. Gasparian, *Phys. Status Solidi B* **2000**, *218*, 151.
[5] A. E. C. Palmqvist, B. B. Iversen, E. Zanghellini, M. Behm, G. D. Stucky, *Angew. Chem.* **2004**, *116*, 718; *Angew. Chem. Int. Ed. Angew. Chem. Int. Ed.* **2004**, *43*, 700.
[6] F. Liebau, *Microporous Mesoporous Mater.* **2004**, *70*, 103.
[7] J. Lin, G. J. Miller, *J. Solid State Chem.* **1994**, *113*, 296.

  

[8] J.-S. Jung, B. Wu, E. D. Stevens, C. J. O'Connor, *J. Solid State Chem.* **1992**, *94*, 362.
[9] X. Wang, F. Liebau, *Acta Crystallogr. Sect. B* **1996**, *52*, 7.
[10] F. Starrost, O. Tiedje, W. Schattke, J. Jockel, U. Simon in *Host–Guest Systems Based on Nanoporous Crystals* (Eds.: F. Laeri, F. Schüth, U. Simon, M. Wark), Wiley-VCH, Weinheim, **2003**, p. 451.
[11] X. Wang, F. Liebau, *Z. Kristallogr.* **1999**, *214*, 820.
[12] F. Rocker, W. Tremel, *Z. Anorg. Allg. Chem.* **2001**, *627*, 1305.
[13] P. Larson, S. D. Mahanti, M. G. Kanatzidis, *Phys. Rev. B* **2000**, *61*, 8162.
[14] F. Liebau, *Microporous Mesoporous Mater.* **2003**, *58*, 15.
[15] J. Rouquerol, D. Avnir, C. W. Fairbridge, D. H. Everett, J. M. Haynes, N. Pernicone, J. D. F. Ramsay, K. S. W. Sing, K. K. Unger, *Pure Appl. Chem.* **1994**, *66*, 1739.
[16] L. B. McCusker, F. Liebau, G. Engelhardt, *Pure Appl. Chem.* **2001**, *73*, 381.
[17] R. Patschke, M. G. Kanatzidis, *Phys. Chem. Chem. Phys.* **2002**, *4*, 3266.
[18] C. Kittel, *Introduction to Solid-State Physics*, 7th ed., Wiley, New York, **1996**.
[19] W. Z. Shen, *Int. J. Infrared Millimeter Waves* **2002**, *23*, 61.
[20] L. J. Farrugia, *J. Appl. Crystallogr.* **1999**, *32*, 837.

  